Where in the underwater world am I?

Towards underwater Simultaneous Localization And Mapping using Sonar and inertial sensing.

BY

B.KNOOK

JANUARY 2019

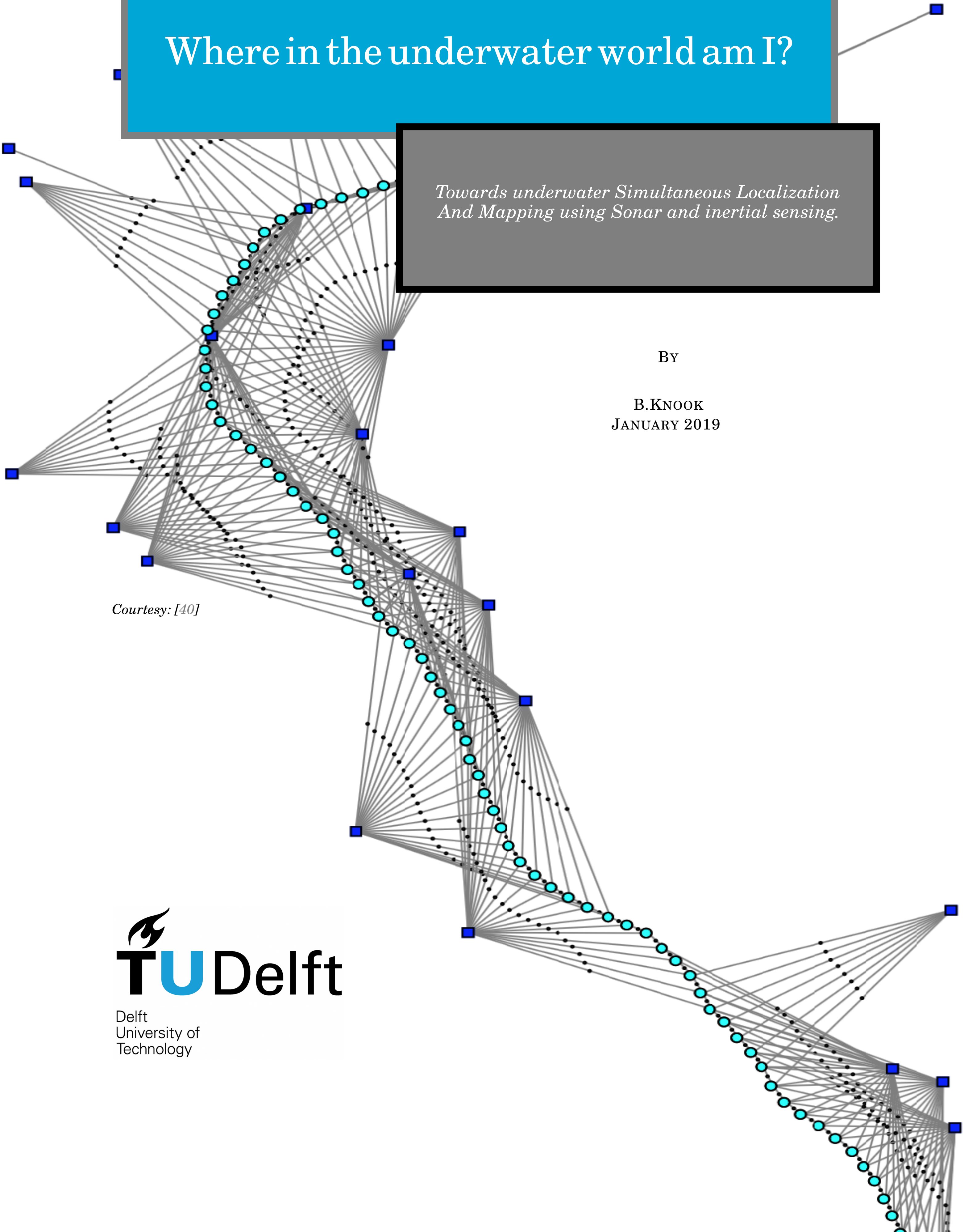

Courtesy: [40]

Delft University of Technology

Where in the underwater world am I?

Towards underwater Simultaneous Localization And Mapping using Sonar and inertial sensing.

By

BASTIAAN KNOOK

JANUARY 08, 2019

An investigation in fulfilment of the requirements in order to obtain the degree of

MASTER OF SCIENCE

at the

FACULTY OF MECHANICAL, MARITIME AND MATERIALS ENGINEERING (3ME), DELFT UNIVERSITY OF TECHNOLOGY

Supervisors :	Prof. dr. ir. C. van Rhee	Prof. dr. ir. P. P. Jonker
Thesis committee:	Prof. dr. ir. C. van Rhee	Prof. dr. ir. P. P. Jonker
	Dr. ir. G.H. Keetels	Dr. ir. J.F.P. Kooij

TU Delft

Delft
University of
Technology

Preface

This research is written in fulfilment of a MSc. double degree in both Offshore and Dredging Engineering and BioMechanical Engineering at the Delft University of Technology. In parallel with this study a separate paper is written, reviewing the state of the art in Simultaneous Localization And Mapping in the structured underwater domain.

Delft University of Technology
Bastiaan Knook
January 08, 2019

Author's declaration

I declare that this thesis was arranged confirming to the requirements of TU Delft its regulations and code of practice for Master programmes and such has not been submitted for any other academic purpose. Except where indicated by specific reference in the text, it is the author's own work. Labour done in collaboration with, or with the assistance of others, is indicated as such. Any views expressed in the manuscript are those of the author.

SIGNED: Bastiaan Knook
PLACE: Hardinxveld-Giessendam
DATE: January 08, 2019

Abstract

Our world is rapidly changing, leading to various technological achievements in diverse areas of expertise. Among the most evolving are autonomous robots, machines and vehicles, enormously extending human capabilities. While this trend became quite familiar for land-based vehicles, innovations in the underwater domain lag behind, mainly due to the harsh environmental conditions encountered. This in large contrast with worldwide growing needs for autonomous underwater solutions, like dredging. Nevertheless, for underwater vehicles becoming autonomously, various technological challenges must be overcome. The most essential one is finding a proper answer to the question; *where in the underwater world am I?*

Autonomous robots are usually be able to operate in complex environments using external reference systems such as Global Positioning System (GPS) to locate themselves inside their environment. However, these are not accessible in underwater applications, since water strongly attenuates electromagnetic signals, notably GPS. Hence, various alternative methods for Simultaneous Localization And Mapping (SLAM) for underwater applications are employed, among which the method of anchoring inertial measurements on environmental landmarks, perceived with an exteroceptive Sonar. The ultimate goal of this procedure is to correct for errors in the inertial measurements, using the environmental perception available in the Sonar scans. Nevertheless, due to practical underwater issues, it still is not readily available and even barely investigated in open scientific research. This thesis aims at the development of an underwater localization algorithm, using onboard inertial sensors and Sonar.

The overall system design consists of several individual software procedures, executing certain assignments, together ultimately solving for the localization task. The developed system was tested using ground truth in form of a real-world dataset obtained several years ago in an abandoned marina. This showed that most individual procedures were able to provide good results, while having a low computational complexity in relation to online operations. However, it is quite a challenge to obtain results accurate enough to properly correct for positional errors, by using the designed system. Although showing potential, it still is not entirely decent in terms of accuracy and computational burden. This is likely due to the sparsity of the extracted Sonar measurements. Data is lacking to further verify the system, hence several questions remain open regarding its universal applicability in case of different scenarios, dynamic environments and long trajectories.

In this context, more in-depth research is needed into the algorithms that are influenced by the Sonar measurements, to increase the accuracy of the overall system, while gaining more insight in its computational behaviour. Additionally, also more real-world experiments are essential, to extensively verify the designed system. In conclusion, the results showed that it is possible to correct for inertial errors, using the system developed. Furthermore, it demonstrates that most procedures individually produce good results in real-time. Hence, this study can be seen as a positive step in the right direction, forming a basis for future research in solutions that are generically applicable in online real underwater world operations.

For confidentiality reasons this page is not displayed.

For confidentiality reasons this page is not displayed.

For confidentiality reasons this page is not displayed.

For confidentiality reasons this page is not displayed.

For confidentiality reasons this page is not displayed.

For confidentiality reasons this page is not displayed.

1-NN	One Nearest Neighbour
RANSAC/GD	RANdom SAmple Consensus/Gaussian Determination
Sonar	SOund Navigation And Ranging

Chapter 1

Introduction

Our world nowadays is rapidly changing, leading to various technological achievements in diverse areas of expertise. Among the most evolving are autonomous robots, machines and vehicles, enormously extending human capabilities. While this trend already became quite familiar for land-based vehicles, innovations in the underwater domain lag behind, mainly due to harsh environmental conditions encountered. This in large contrast with worldwide growing needs for autonomous underwater solutions, which is even emphasized by the tendency to continuously tighten up sustainability policies around the globe. Hence, Autonomous Underwater Vehicles (AUV)s entirely fit in the goals of subsea industries, waterway authorities and so on to be most competitive, innovative and sustainable. Nevertheless, for underwater vehicles becoming autonomously, various technological challenges must be overcome. The most essential one is finding a proper answer to the question; *where in the underwater world am I?*, before reasoning about navigational questions like; *(1) to which location am I going?* and *(2) in what manner shall I get there?* [12, 75, 111].

Autonomous robots are usually able to operate in complex environments using external reference systems such as Global Positioning System (GPS) to locate themselves inside their environment. However, these are not accessible in underwater applications, since water strongly attenuates electromagnetic signals, notably GPS [76]. Hence, various alternatives are commonly employed, most frequently in form of dead reckoning using so-called proprioceptive sensors like a compass, Inertial Measurement Unit (IMU) and so on [50, 53, 88]. These alternatives are commonly used to estimate the position of an AUV, by integrating inertial data over time from a known initial position, whether or not augmented with velocity predictions using a Doppler Velocity Log (DVL) [99]. However, a major disadvantage is the accumulated error, because of integration drift. Any measurement error, no matter how small, accumulates inside the continuous integration of acceleration towards velocity and location. Hence, a constant acceleration error becomes linear in velocity and quadratic in location [120]. Since a new estimate depends on its previous one, the error is cumulative and evolves unbounded with distance travelled [88, 99]. Consequently, implying a large inaccuracy in estimated position over time, making dead reckoning impractical for long-term navigation.

To reduce this drift, inertial systems can be combined somehow with other sensors and methodologies. The first approach is positioning through an external infrastructure, applying independent acoustic transponders and modems [76, 88]. Techniques belonging to this category are based on Time-Of-Flight (TOF) measurements of signals emitted from external predeployed acoustic beacons or modems. Devices belonging to this category are, among others, Long Baseline (LBL), Short Baseline (SBL), Ultra-Short Baseline (USBL) and GPS Intelligent Buoys (GIB)s [88, 99]. Nonetheless, making use of this approach brings forth several disadvantages. When using a support ship, as is common in navigation techniques based on SBL and USBL systems, it must precisely follow the AUV to ensure coverage [99]. Moreover, although LBL mostly delivers high accuracy results, only small areas can be covered at once, otherwise the AUV becomes out of range. Together with the procedure of deployment, calibration and recovery, it is clear that these types of operations are costly in terms of time and expenditures [50, 99]. Furthermore, effective deployment of acoustic beacons can be quite challenging in particular scenarios, depending on the seabed relief [99]. Sometimes it also might be not doable because of the acoustic noise already present in an environment, like for example signals due to the shipping industry. At last, for vehicles becoming autonomously, they should be able to localize in whatever kind of conditions, thereby only using onboard sensor systems without the need of external infrastructures [99].

Correction through environmental landmarks perceived with an exteroceptive sensor is another approach, known as Simultaneous Localization And Mapping (SLAM) [1] [76]. Generally, a broad spectrum of sensory devices is available, varying from optical cameras or Light Amplification by Stimulated Emission of Radiation (Laser) scanners, such as Light Detection And Ranging (LiDAR), up to acoustic imaging systems in form of SOund Navigation And Ranging (Sonar). By solving for the fundemental SLAM issue, it is doable to constraint the drift and localize the AUV more accurately in its environment, solely based on proprioceptive and exteroceptive sensors. More formally, it encompasses the synchronous estimation of robotic poses using proprioceptive measurements and the construction of an environmental model by exteroceptive readings [44, 53, 88]. While robotic poses consist of location and orientation, the environmental model or map describes surroundings by representing diverse aspects of interest, like locations of landmarks or objects, characterized by their features. Obviously this method has its limitations in the unstructured domain, because environmental characteristics are mostly lacking. However, numerous marine activities, wherein AUVs can significantly contribute, take place in relatively shallow and structured environments. Therefore, arriving at underwater SLAM which, due to practical issues, is still not readily available and even barely investigated in open scientific research. Hence, this thesis aims at the development of an underwater localization algorithm, using onboard sensors in form of an IMU, DVL and imaging Sonar.

1.1 The concept of SLAM

SLAM examines the problem where a mobile autonomous vehicle or robot is placed in an unknown environment and at an unknown location to explore it, having only onboard proprioceptive and exteroceptive sensors at its disposal [44, 53, 78]. By fusing sensory data, it tries to build a consistent environmental map, while simultaneously computing its location in this map. The SLAM procedure is also known as the chicken-and-egg problem, being a causality dilemma since consistent environmental maps are needed for proper localization, while simultaneously accurate robot positions are a must in collecting these maps

[1] Or Concurrent Mapping And Localization (CML) [88, 112, 114].

For confidentiality reasons this page is not displayed.

For confidentiality reasons this page is not displayed.

For confidentiality reasons this page is not displayed.

For confidentiality reasons this page is not displayed.

For confidentiality reasons this page is not displayed.

For confidentiality reasons this page is not displayed.

For confidentiality reasons this page is not displayed.

For confidentiality reasons this page is not displayed.

For confidentiality reasons this page is not displayed.

For confidentiality reasons this page is not displayed.

For confidentiality reasons this page is not displayed.

For confidentiality reasons this page is not displayed.

For confidentiality reasons this page is not displayed.

For confidentiality reasons this page is not displayed.

For confidentiality reasons this page is not displayed.

For confidentiality reasons this page is not displayed.

For confidentiality reasons this page is not displayed.

For confidentiality reasons this page is not displayed.

For confidentiality reasons this page is not displayed.

For confidentiality reasons this page is not displayed.

For confidentiality reasons this page is not displayed.

For confidentiality reasons this page is not displayed.

For confidentiality reasons this page is not displayed.

For confidentiality reasons this page is not displayed.

For confidentiality reasons this page is not displayed.

For confidentiality reasons this page is not displayed.

For confidentiality reasons this page is not displayed.

For confidentiality reasons this page is not displayed.

For confidentiality reasons this page is not displayed.

For confidentiality reasons this page is not displayed.

For confidentiality reasons this page is not displayed.

For confidentiality reasons this page is not displayed.

For confidentiality reasons this page is not displayed.

For confidentiality reasons this page is not displayed.

For confidentiality reasons this page is not displayed.

For confidentiality reasons this page is not displayed.

For confidentiality reasons this page is not displayed.

For confidentiality reasons this page is not displayed.

For confidentiality reasons this page is not displayed.

For confidentiality reasons this page is not displayed.

For confidentiality reasons this page is not displayed.

For confidentiality reasons this page is not displayed.

For confidentiality reasons this page is not displayed.

For confidentiality reasons this page is not displayed.

For confidentiality reasons this page is not displayed.

For confidentiality reasons this page is not displayed.

For confidentiality reasons this page is not displayed.

For confidentiality reasons this page is not displayed.

For confidentiality reasons this page is not displayed.

For confidentiality reasons this page is not displayed.

For confidentiality reasons this page is not displayed.

For confidentiality reasons this page is not displayed.

For confidentiality reasons this page is not displayed.

For confidentiality reasons this page is not displayed.

For confidentiality reasons this page is not displayed.

For confidentiality reasons this page is not displayed.

For confidentiality reasons this page is not displayed.

For confidentiality reasons this page is not displayed.

For confidentiality reasons this page is not displayed.

For confidentiality reasons this page is not displayed.

For confidentiality reasons this page is not displayed.

For confidentiality reasons this page is not displayed.

For confidentiality reasons this page is not displayed.

For confidentiality reasons this page is not displayed.

For confidentiality reasons this page is not displayed.

For confidentiality reasons this page is not displayed.

For confidentiality reasons this page is not displayed.

For confidentiality reasons this page is not displayed.

For confidentiality reasons this page is not displayed.

For confidentiality reasons this page is not displayed.

Acknowledgements

I would especially like to thank my beloved girlfriend Sietske, my parents and the rest of my amazing family and close relatives for the love, support and constant encouragement I have gotten over the years. Above all else I thank God for being there during my whole study and graduation process. I would also like to thank my thesis committee members Prof.dr.ir. C. van Rhee, Prof.dr.ir. P.P. Jonker, Dr.ir. G.H. Keetels and Dr.ir. J.F.P. Kooij for all of their guidance through this graduation process; your ideas, discussion and feedback have been absolutely invaluable.

Delft University of Technology
Bastiaan Knook
January 08, 2019

For confidentiality reasons this page is not displayed.

For confidentiality reasons this page is not displayed.

For confidentiality reasons this page is not displayed.

in Figure 4.6. Still the algorithm was much too conservative also removing a lot of bona fide measurements, resulting in quite a loss of detail in each scan. Moreover, the above segmentation process must be applied with caution since it heavily relies on a fixed distance between the robot and its environment, which in addition is assumed to be static. Principally this can be seen as taking into account prior knowledge, expecting the Sonar update rate to be high enough to exclude dynamic surprises. Therefore, the technique is not really desirable and not considered any further in the investigation.

APPENDIX

B

POSE COMPOUNDING OPERATIONS

This appendix briefly explains two concepts commonly used in the literature regarding Simultaneous Localization And Mapping (SLAM) solutions, scan matching procedures, robotics and such. They are closely related to each other and are called the pose compounding and inversion operator. Their mutual relation will be clarified on the basis of mathematical theory. In doing so, Section B.1 discusses the pose compounding operation, while Section B.2 elaborates the inverse operator.

B.1 Compounding operator

Almost everything within robotics has to do with poses. As mentioned earlier, a pose consists of the location and orientation of an object, having its coordinate frame in multiple dimensions. Normally, poses are relative to each other or relative to the world coordinate frame, such describing the position and orientation of one coordinate system with respect to another [105]. In the context of this investigation, a certain Autonomous Underwater Vehicle (AUV) continously obtains new poses when traversing an environment, usually relative to their starting pose referred to as the world coordinate system. In the following two-dimensional (2D) example, consider that the AUV starts at pose $\boldsymbol{x}_w = [x_w, y_w, \theta_w]^T$ [1], whereafter it explores the environment through which the pose varies with $\boldsymbol{\xi} = {}^w\boldsymbol{\xi}_I = [x, y, \theta]^T$ relative to $\boldsymbol{x}_w$ before reaching a new pose $\boldsymbol{x}_I = [x_I, y_I, \theta_I]^T$ [78]. The latter defines the new coordinate [2] system and can be obtained through a certain transformation, the so-called compounding operation or head-to-tail relationship, discussed in among others [78, 105, 107]:

$$\boldsymbol{x}_I = \begin{bmatrix} x_I \\ y_I \\ \theta_I \end{bmatrix} = \boldsymbol{x}_w \oplus \boldsymbol{\xi} = \begin{bmatrix} \boldsymbol{T}_w \\ \boldsymbol{A}_w \end{bmatrix} \tag{B.1}$$

[1] Please note that the poses considered in this appendix are modeled as Random Gaussian Variables (r.g.v.)s in practice. However, for the sake of simplicity its mathematical description is not taken over in this chapter, but instead the poses are assumed to be deterministic.

[2] Usually, an absolute pose represents the position plus orientation of a coordinate frame in a global space, in the 2D case, consisting of x, y coordinates and direction θ [78].

Where $\boldsymbol{T}_w$ takes into account both the rotation [3] and the translation due to AUV motion:

$$\boldsymbol{T}_w = \boldsymbol{R}_w \begin{bmatrix} x \\ y \end{bmatrix} + \begin{bmatrix} x_w \\ y_w \end{bmatrix} = \begin{bmatrix} \cos(\theta_w) & -\sin(\theta_w) \\ \sin(\theta_w) & \cos(\theta_w) \end{bmatrix} \begin{bmatrix} x \\ y \end{bmatrix} + \begin{bmatrix} x_w \\ y_w \end{bmatrix} \tag{B.2}$$

And $\boldsymbol{A}_w$ is defined as [105]:

$$\boldsymbol{A}_w = \theta_w + \theta \tag{B.3}$$

Hence, the coordinates are interconnected by [78]:

$$x_I = x_w + x\cos(\theta_w) - y\sin(\theta_w) \tag{B.4}$$

$$y_I = y_w + x\sin(\theta_w) + y\cos(\theta_w) \tag{B.5}$$

$$\theta_I = \theta_w + \theta \tag{B.6}$$

Generally, a homogeneous transformation can also be established, starting with $\boldsymbol{T}_w$ [38]:

$$\boldsymbol{T}_w \rightarrow \boldsymbol{T}_h = \begin{bmatrix} \cos(\theta_w) & -\sin(\theta_w) & x_w \\ \sin(\theta_w) & \cos(\theta_w) & y_w \\ 0 & 0 & 1 \end{bmatrix} \begin{bmatrix} x \\ y \\ 1 \end{bmatrix} = \boldsymbol{R}_h \begin{bmatrix} x \\ y \\ 1 \end{bmatrix} = \begin{bmatrix} x_I \\ y_I \\ 1 \end{bmatrix} \tag{B.7}$$

Consequently, compounding two poses $C = D \oplus E$ equals the multiplication of their corresponding homogeneous coordinate matrices $R_D R_E$, resulting in the homogeneous matrix of the new pose C [11]. Moreover, note that the compounding operation is associative and not commutative [78]. Normally, it is used to compute the location of a mobile robot after a serie of relative movements [107].

B.2 Inversion operator

In general, a new composite transformation can be formed by computing a sequence of previous relative transformations, using Eq. (B.1). However, frame relationships are directed [107], in close analogy to the pose-graph representation. Meaning that sometimes one needs to perform a backwards computation against the forward pose or graph direction to establish a new pose [105, 107]. This reversal can be easily captured by a mathematical expression called the inverse transformation [107]:

$$\boldsymbol{x}_{w^{-1}} = \ominus \boldsymbol{x}_w = \begin{bmatrix} -x_w\cos(\theta_w) - y_w\sin(\theta_w) \\ x_w\sin(\theta_w) - y_w\cos(\theta_w) \\ -\theta_w \end{bmatrix} \tag{B.8}$$

In a similar manner the inverse of compounding can be established, wherein the relative pose is determined given two poses [78]:

$$\boldsymbol{\xi} = {}^I\boldsymbol{\xi}_w = \boldsymbol{x}_I \ominus \boldsymbol{x}_w \tag{B.9}$$

Whose computation results in the following equations:

$$x = (x_I - x_w)\cos(\theta_w) + (y_I - y_w)\sin(\theta_w) \tag{B.10}$$

$$y = -(x_I - x_w)\sin(\theta_w) + (y_I - y_w)\cos(\theta_w) \tag{B.11}$$

$$\theta = \theta_I - \theta_w \tag{B.12}$$

[3] By means of a $2x2$ rotation matrix around the z-axis or yaw parametrized by θ_w.

Given this relationship it can be verified that the tail-to-tail combination $(\ominus D) \oplus E = E \ominus D$. For more information regarding pose compounding, derivations in case of three dimensions or rigid-body theory, the interested reader is referred to one of the excellent sources [38, 78, 105, 107].

For confidentiality reasons this page is not displayed.

For confidentiality reasons this page is not displayed.

For confidentiality reasons this page is not displayed.

For confidentiality reasons this page is not displayed.

For confidentiality reasons this page is not displayed.

For confidentiality reasons this page is not displayed.

For confidentiality reasons this page is not displayed.

For confidentiality reasons this page is not displayed.

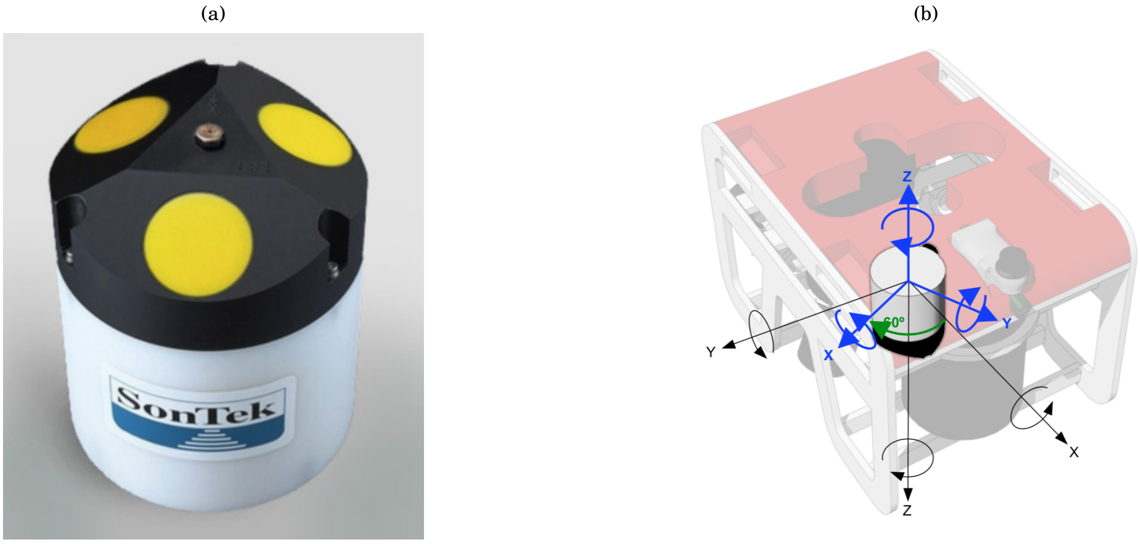

FIGURE D.1. *(a) Visualization of the Sontek Argonaut DVL. (b) Positioning of the DVL sensor inside the operating vehicle. The first photo is reproduced from [94], while the second is obtained from [92].*

The operating frequency of the system is 1500 $[kHz]$, while the output rate is around 1.5 $[Hz]$ [1] due to acoustic limitations [94]. The device is mounted inside the operating platform, having its sensor coordinate frame with respect to the vehicle frame as depicted in Figure D.1(b). The blue axes represent the local sensor's frame [2], in which positive measurements have been established, while the black axes correspond to the local vehicle reference coordinate frame. Given this information, one is able to construct a rigid-body transformation resulting in a transformed vector of the form:

$$\boldsymbol{T}_{D\rightarrow R} = \boldsymbol{R}_{D\rightarrow R}\{D\} + \boldsymbol{t}_{D\rightarrow R} \tag{D.1}$$

In which rotation matrix $\boldsymbol{R}_{D\rightarrow R}$ and vector $\boldsymbol{t}_{D\rightarrow R}$ respectively take care of the rotation and translation of the data in the sensor frame $\{D\}$ towards the local vehicle frame $\{R\}$.

D.2 Motion Reference Unit

The Xsens MTi is a small low-cost and gyro-enhanced Motion Reference Unit (MRU) providing acceleration, attitude, heading and rate of turn measurements all in 3DOF [92, 94]. The output rate of the device is around 10 $[Hz]$. However, because of the small accelerations experienced by the vehicle, their linear measurements in 3DOF became inaccurate [94]. Nevertheless, angular estimations seem to be more reliable. Moreover, the output rate is much higher compared to the DVL. Hence, this sensor is the main source for the prediction of the vehicle's attitude and heading information [94]. Figure D.2(a) shows the MTi device, while Figure D.2(b) describes its position with respect to the operating platform. The blue and black coordinate frames are completely similar to the ones explained in Section D.1, except for the former

[1] Although some internal sensors are able to produce measurements at higher rates [94].
[2] Consisting of both positive linear and angular directions.

For confidentiality reasons this page is not displayed.

For confidentiality reasons this page is not displayed.

For confidentiality reasons this page is not displayed.

For confidentiality reasons this page is not displayed.

For confidentiality reasons this page is not displayed.

For confidentiality reasons this page is not displayed.

For confidentiality reasons this page is not displayed.

For confidentiality reasons this page is not displayed.

For confidentiality reasons this page is not displayed.

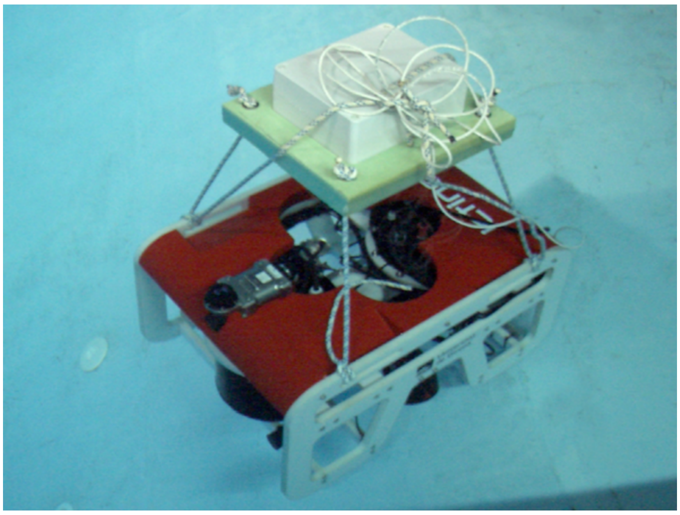

FIGURE D.11. *Photograph of the operating platform and buoy, wherein the DGPS is located. The buoy is fixed by four anchor-points to ensure it will always be located directly above the vehicle. The figure is reproduced from [92].*

Appendix

E

Image processing

This appendix briefly describes the two main mathematical techniques being employed in the beam segmentation procedures, as explained in Section 3.3 and Appendix A. In doing so, the *Gaussian blur filter* as particular type of spatial filtering is explained in Section E.1, whereas Section E.2 discusses the *Erode* operation.

E.1 Filtering in spatial domain

Presumably the most used categorie nowadays is filtering in the spatial domain using a two-dimensional (2D) sliding window, being equivalent to filtering in the frequency domain [30]. Spatial filters make use of a pixel-by-pixel transformation of an image, not only depending on the pixel value being processed, but also on its neighbouring pixel values [30, 59]. Hence, this procedure is also known as neighborhood processing. It defines a center pixel for which an operation is performed, by taking into account predefined neighboring pixels. Generally, the operation is presented by a matrix with dimensions equal to the amount of predefined neighboring pixels. By computing the operation stated in the matrix [1], a new value for the center pixel is obtained. By sliding the matrix over a two-dimensional image, the process is repeated for each pixel within it. An example of the process is visualized in Figure E.1. The matrix or 2D sliding window is also known as filter, mask or kernel [30, 59]. The first metonym orginates from functions in the frequency domain. For convenience, it is commonly named a spatial filter to emphasis its spatial operation [59]. The calculation of a new value for the center pixel can depend in a linear or non-linear fashion on its neighboring pixel values in combination with specific weighting coefficients [30, 102]. A mathematical expression of a spatial linear filter g is given by [2] [108]:

$$g(i,j) = \sum_{k=-a}^{a} \sum_{l=-b}^{b} w(k,l) f(i+k, j+l) \tag{E.1}$$

[1] Which is generally a linear combination of its neighboring pixel values with specific weigth coefficients [102].

[2] Note that Eq. (E.1) is a cross-correlation operation $H \otimes F$ rather than a convolution $H * F$ in which the kernel is flipped both horizontally and vertically [108].

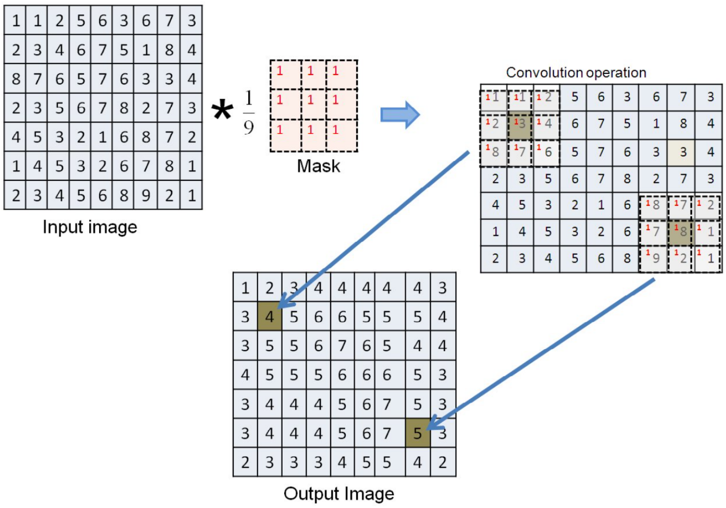

FIGURE E.1. *Visualization of a spatial filter, as applied to a random two-dimensional image. This figure is duplicated from [30].*

In which g is the output after filtering, f equals a digital input image of size MxN and w represents the filter kernel of size $w_m x w_n$. The dummy variables are $a = \frac{w_n - 1}{2}$ and $b = \frac{w_n - 1}{2}$. Linear filtering in the spatial domain is basically an application of the convolution operator [51, 59, 90]. Filter performance depends, among others, on kernel dimensions which must be specified by the user. Different sizes result in diverse output images, based on the level of noise and intended result one wants to obtain. However, the kernel always needs an odd number of pixels in rows and columns to ensure a single unique center pixel [30]. Usually, for a 2D image a square kernel with sizes of $3x3$, $5x5$, $7x7$ pixels gives satisfactory results [102]. The edges of an image must be treated carefully, since the kernel is partly outside the image space [59]. Several approaches exist to solve for this issue. One solution is to pad the outer edges of an image, by adding zeros around the image at the expense of a slightly darker outer edge. Another preferable solution would be to mirror the pixel values of an image around its edges [59]. In this way, no new information is added to an image and the edges will not be distorted. This approach is equivalent to ignoring the values where an image and the kernel do not overlap, albeit easier to implement.

E.1.1 Square Gaussian weighted average filter

One low-pass filtering technique is the square Gaussian weighted average filter, sigma filter or *Gaussian blur filter* developed to improve on the capabilities of the mean kernel filter [3, 73, 89, 102]. Rather than defining coefficients equal to $\frac{w(k,l)}{w_m w_n} = \frac{1}{w_m w_n} | \forall k \in [-a,a] \cap l \in [-b,b]$, as is the case for average filtering, they are sampled from a Gaussian bell whose width is a user-defined number of standard deviations [66, 102]:

$$g(i,j) = \sum_{k=-a}^{a} \sum_{l=-b}^{b} w(k,l) f(i-k, j-l) \tag{E.2}$$

with:

$$w(k,l) = \frac{1}{2\pi\sigma^2} e^{-\frac{k^2+l^2}{2\sigma^2}} \tag{E.3}$$

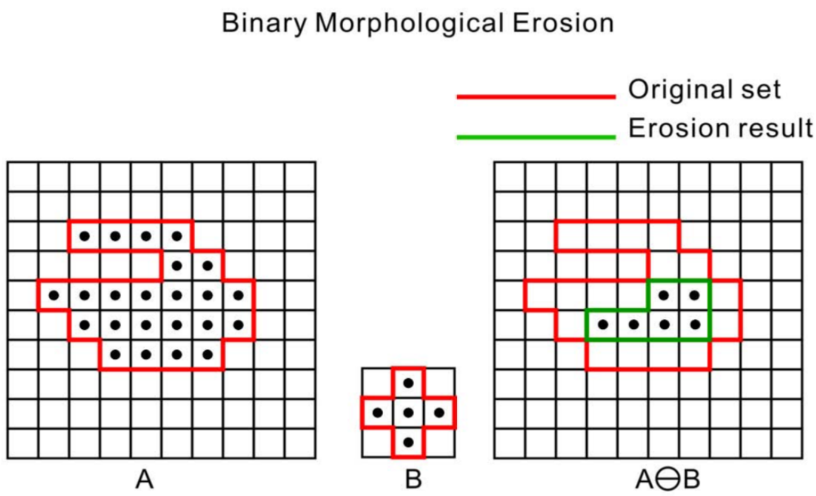

FIGURE E.2. *A binary image A is eroded by a cross-shaped structuring element B. The figure is reproduced from [126].*

Where σ is the standard deviation. The normalized kernel coefficients are related to the specified width by the probability density region covered. For example, two standard deviations cover 95% of the Gaussian bell, wherein the coefficients will be computed [102]. Main idea is that pixels closely located to the central one more likely belong to the same image region. Consequently, neighboring pixels located closest to the central have heigher weighting coefficients in the average calculation, whereas pixels further away recieve lower weights [102].

E.2 Morphological operations

This section briefly explains the morphological erosion operator. Commonly, its input is a binary image consisting of only two Boolean values for each pixel, namely zero or one [126]. It makes use of a spatial window in analogy to Section E.1. However, the official term used to describe morphology is a binary structuring element, rather than a kernel or window [30, 126]. It interacts with a given image and influences its geometric structure [126]. Selecting the proper shape or size for it, depends on the shapes and sizes of the targets in the image [126]. Mostly used are octagonal, disk-shaped, rectangle, line segment, diamond or square structuring elements. The morphological operation places the structuring element over each pixel in a binary image, whereafter it performs a logical test [30]. Hence, it affects the image and is able to effectively reduce noise and enhance objects. Let A be the input image and B the structuring element. The definition of erosion is [73, 126]:

$$A \ominus B = \bigcap_{b \in B} A_{-b} \rightarrow A \ominus B(m,n) = min\{A(m+i,n+j)|(i,j) \in B\} \tag{E.4}$$

Wherein $\ominus$ is the Minkowski subtraction [73] and $\bigcap$ stands for the intersection between the structuring element and the image. Thus erosion shrinks objects, separates fragemented characteristics and removes small targets, by combining both sets due to the vector subtraction of all elements b [126]. The result of an erosion process is displayed in Figure E.2.

BIBLIOGRAPHY

[1] Allawi, Z. and Abdalla, T. [2014], 'An Accurate Dead Reckoning Method based on Geometry Principles for Mobile Robot Localization', *International Journal of Computer Applications* **95**(13), 21–25.

[2] Allotta, B., Conti, R., Costanzi, R., Fanelli, F., Gelli, J., Meli, E., Monni, N., Ridolfi, A. and Rindi, A. [2017], 'A low cost autonomous underwater vehicle for patrolling and monitoring', *Proc. of the Intitution of Mechanical Engineers, Part M: Journal of Engineering for the Maritime Environment* **231**(3), 740–749.

[3] Argenti, F., Lapini, A., Bianchi, T. and Alparone, L. [2013], 'A Tutorial on Speckle Reduction in Synthetic Aperture Radar Images', *IEEE Geoscience and Remote Sensing Magazine* **1**(3), 6–35.

[4] Bailey, T. and Durrant-Whyte, H. [2006], 'Simultaneous localisation and mapping (SLAM): part II State of the Art', *IEEE robotics & automation magazine* **13**(3), 108–117.

[5] Bar-Shalom, Y. and Fortmann, T. [1987], *Tracking and Data Association*, **ISBN: 0-120-79760-7**, Academic Press Professional, Inc., San Diego, CA, USA.

[6] Baruch, A., Kamber, E., Arbel, I., Braginsky, B. and Guterman, H. [2016], 'Navigation approaches for hovering autonomous underwater vehicles', *International Conference on the Science of Electrical Engineering (ICSEE)* pp. 1–5.

[7] Belongie, S. and Malik, J. [2000], 'Matching with shape contexts', *IEEE Proc. Workshop on content-based access of image and video libraries* pp. 20–26.

[8] Belongie, S., Malik, J. and Puzicha, J. [2002], 'Shape matching and object recognition using shape contexts', *IEEE Transactions on Pattern Analysis and Machine Intelligence* **24**(24), 509–522.

[9] Bengtsson, O. and Baerveldt, A. [2003], 'Robot localization based on scan-matching-estimating the covariance matrix for the IDC algorithm', *Robotics and Autonomous Systems* **44**(1), 29–40.

[10] Besl, P. and McKay, N. [1992], 'A method for registration of 3-D shapes', *IEEE Transactions on Pattern Analysis and Machine Intelligence* **14**(2), 239–256.

[11] Blanco, J. [2008], Derivation and implementation of a full 6D EKF-based Solution to Bearing-Range SLAM, Technical report, University of Málaga; Perception and mobile robots research group.

[12] Borenstein, J., Everett, H., Feng, L., Lee, S. and Byrne, R. [1996], Where am I, Technical report, Prepared by the University of Michigan; For the ORNL D&D Program and U.S. department of energy's.

For confidentiality reasons this page is not displayed.

For confidentiality reasons this page is not displayed.

For confidentiality reasons this page is not displayed.

For confidentiality reasons this page is not displayed.

For confidentiality reasons this page is not displayed.

[101] Santos, M., Ribeiro, P., nez, P. N., Drews-Jr, P. and Botelho, S. [2017], 'Object Classification in Semi Structured Environment Using Forward-Looking Sonar', *Sensors* **10**(2235).

[102] Sauter, D. and Parson, L. [1994], 'Spatial filtering for speckle reduction, contrast enhancement and texture analysis of GLORIA images', *IEEE Journal of Oceanic Engineering* **19**(4), 563–576.

[103] Shen, Y., Zhang, H., Yan, T. and Liu, Y. [2015], 'Autonomous Navigation Based on SEIF with Consistency Constraint for C-Ranger AUV', *Hindawi Mathematical Problems in Engineering* **2015**(Article ID 752360), 1–12.

[104] Silver, D., Bradley, D. and Thayer, S. [2004], 'Scan matching for flooded subterranean voids', *IEEE Conference on robotics, automation and mechatronics* .

[105] Smith, R. and Cheeseman, P. [1986], 'On the Representation and Estimation of Spatial Uncertainty', *The International Journal of Robotics Research* **5**(4), 56–68.

[106] Smith, R., Self, M. and Cheeseman, P. [1988], A stochastic map for uncertain spatial relationships, *in* O. Faugeras and G. Giralt, eds, 'Robotics Research, the fourth International Symposium', The MIT Press.

[107] Smith, R., Self, M. and Cheeseman, P. [1990], Estimating Uncertain Spatial Relationships in Robotics , *in* L. N. K. Lemmer, J.F., ed., 'Uncertainty in Artificial Intelligence', Vol. 5 of *Machine Intelligence and Pattern Recognition*, Springer-Verlag, pp. 435–461.

[108] Snavely, N. [2018], 'Cs6670: Computer vision, lecture 1: images and image filtering', **Online** [Last accessed: January 27, 2018].
URL: *https://www.coursehero.com/file/5962397/lec01-filter/*

[109] Solá, J. [2017], Course on SLAM, Technical report, Institute de Robótica i Informática Industrial, Universitat Politéchnica de Catalunya Barcelonatech.

[110] Song, S., Herrmann, J., Si, B., Liu, K. and Feng, X. [2017], 'Two-dimensional forward-looking sonar image registration by maximization of peripheral mutual information', *International Journal of Advanced Robotic Systems* pp. 1–17.

[111] Sünderhauf, N. [2012], Robust Optimization for Simultaneous Localization and Mapping, PhD thesis, Technischen Universität Chemnitz.

[112] Tardós, J., Neira, J., Newman, P. and Leonard, J. [2002], 'Robust Mapping and Localization in Indoor Environments Using Sonar Data', *The International Journal of Robotics Research* **21**(4), 311–330.

[113] team OpenCv [n.d.], 'Opencv library', **Online** [Last accessed: Oktober 03, 2018].
URL: *https://opencv.org*

[114] Thrun, S. [2001], A Probabilistic Online Mapping Algorithm for Teams of Mobile Robots, Technical report, Carnegie Mellon university, school of computer science.

[115] Thrun, S., Burgard, W. and Fox, D. [2006], *Probabilistic Robotics; From Intelligent Robotics and Autonomous Agents series*, **ISBN: 978-0-262-20162-9**, The MIT Press.

For confidentiality reasons this page is not displayed.